

See discussions, stats, and author profiles for this publication at: <https://www.researchgate.net/publication/12682405>

# Synthesis, and cytotoxic activity of some novel indolo[2,3-b]quinoline derivatives: DNA topoisomerase II inhibitors

ARTICLE in BIOORGANIC & MEDICINAL CHEMISTRY · DECEMBER 1999

Impact Factor: 2.79 · DOI: 10.1016/S0968-0896(99)00200-X · Source: PubMed

---

CITATIONS

34

READS

50

## 9 AUTHORS, INCLUDING:



Lukasz Szymon Kaczmarek

Instytut Farmaceutyczny

169 PUBLICATIONS 801 CITATIONS

[SEE PROFILE](#)



Waclaw Andrzej Sokalski

Wroclaw University of Technology

119 PUBLICATIONS 2,352 CITATIONS

[SEE PROFILE](#)



Janusz Boratyński

Polish Academy of Sciences

82 PUBLICATIONS 853 CITATIONS

[SEE PROFILE](#)



Ewa Marcinkowska

University of Wroclaw

48 PUBLICATIONS 756 CITATIONS

[SEE PROFILE](#)



Pergamon

# Synthesis, and Cytotoxic Activity of Some Novel Indolo[2,3-*b*]quinoline Derivatives: DNA Topoisomerase II Inhibitors

Łukasz Kaczmarek,<sup>a</sup> Wanda Peczyńska-Czoch,<sup>b,\*</sup> Jarosław Osiadacz,<sup>c</sup> Marian Mordarski,<sup>c</sup> W. Andrzej Sokalski,<sup>d</sup> Janusz Boratyński,<sup>e</sup> Ewa Marcinkowska,<sup>e</sup> Halina Glazman-Kuśnierszczak,<sup>e</sup> and Czesław Radzikowski<sup>e</sup>

<sup>a</sup>Pharmaceutical Research Institute, Rydygiera 8, 01-783 Warsaw, Poland

<sup>b</sup>Institute of Organic Chemistry, Biochemistry & Biotechnology, Wrocław University of Technology,  
Wybrzeże Wyspianskiego 27, 50-370 Wrocław, Poland

<sup>c</sup>Department of Microbiology, Institute of Immunology and Experimental Therapy, Polish Academy of Sciences,  
Weigla 12, 53-114 Wrocław, Poland

<sup>d</sup>Institute of Theoretical and Physical Chemistry, Wrocław University of Technology,  
Wybrzeże Wyspianskiego 27, 50-370 Wrocław, Poland

<sup>e</sup>Department of Tumor Immunology, Institute of Immunology and Experimental Therapy,  
Polish Academy of Sciences, Weigla 12, 53-114 Wrocław, Poland

Received 16 March 1999; accepted 26 May 1999

**Abstract**—A series of new 5*H*-indolo[2,3-*b*]quinoline derivatives bearing methoxy and methyl groups at C-2 and C-9 was synthesized (according to the modified Graebe–Ullmann reaction). These compounds were evaluated for their antimicrobial and cytotoxic activity and tested as inhibitors of DNA topoisomerase II. Lipophilic and calf thymus DNA binding properties of these compounds were also established. In the SAR studies we used quantum-mechanical methodology to analyze the molecular properties of the drugs. All of the 5*H*-indolo[2,3-*b*]quinolines tested were found to inhibit the growth of Gram-positive bacteria and pathogenic fungi at MIC ranging between 2.0 and 6.0 μM. They showed also cytotoxic activity in vitro against several human cancer cell lines of different origin (ID<sub>50</sub> varied from 0.6 to 1.4 μM), and stimulated the formation of topoisomerase-II-mediated pSP65 DNA cleavage at concentration between 0.2 and 0.5 μM. The most active indolo[2,3-*b*]quinolines which had the greatest contribution to the increase in the *T<sub>m</sub>* of DNA displayed also the highest DNA binding constants and the highest cytotoxic activity. The differences in DNA binding properties and cytotoxic activity seem to be more related to steric than electrostatic effects. © 1999 Elsevier Science Ltd. All rights reserved.

## Introduction

In our previous papers we reported the synthesis and preliminary evaluation of indolo[2,3-*b*]quinoline derivatives which appeared to be a new class of cytotoxic DNA intercalators and topoisomerase II inhibitors.<sup>1,2</sup> Owing to the novelty of the indolo[2,3-*b*]quinoline core, a synthetic program was undertaken to explore the structure–activity relationship with the objective to increase the potency and specificity of the action of

these compounds. We found that only derivatives belonging to the 5*H*-series (i.e. those bearing a methyl group on the pyridine nitrogen, which stabilizes the positive charge of the molecule) showed significant activity against prokaryotic and eukaryotic organisms, increased calf thymus DNA denaturation temperature (*T<sub>m</sub>*) and stimulated the formation of calf thymus topoisomerase II mediated DNA cleavage.<sup>3</sup>

In our former SAR study we found that none of the analogous indolo[2,3-*b*]quinolines belonging to the 6*H*-series (i.e. those lacking in a methyl group on the pyridine nitrogen) was active in appropriate tests.<sup>3</sup> As part of our structure–activity program, which aimed at obtaining novel indolo[2,3-*b*]quinolines with improved

Key words: Indolo[2,3-*b*]quinolines; cytotoxic agents; topoisomerase II inhibitors; quantum chemical calculations.

\* Corresponding author. Tel.: +4871-320-24-59; e-mail: peczynska@kchf.ch.pwr.wroc.pl

therapeutic potential, we synthesized the methoxy and methyl-methoxy derivatives of our lead compound: 5-11-dimethyl-5*H*-indolo[2,3-*b*]quinoline (DiMIQ, compound **8**) and evaluated them as cytotoxic agents in vitro and in vivo. The same derivatives were also investigated as topoisomerase II inhibitors. With the aim to recognize the contribution of the methoxy and methyl groups at C-2 and/or C-9 to the activity of 5*H*-indolo[2,3-*b*]quinolines, we selected three sets of compounds for preparation: (i) substituted with a methoxy group at C-2; (ii) bearing this substituent at C-9; (iii) disubstituted at C-2 and C-9 with methoxy, methyl and methoxy or methoxy and methyl groups, respectively. The compounds obtained were evaluated for their antimicrobial properties and cytotoxicity against several human cell lines in vitro. Investigated was also the ability of these compounds to induce in vitro the formation of calf thymus DNA topoisomerase II mediated cleavable complexes. Additionally, we determined the lipophilicity,  $pK_a$  values, DNA binding constant ( $K_{app}$ )<sup>4</sup> and thermal stability of the indolo[2,3-*b*]quinoline-DNA complex ( $\Delta T_m$ ). In the SAR study we used the quantum-mechanical methodology to analyze the geometry and the electrostatic properties of the drugs. The geometry of the investigated compounds was optimized, using both ab initio LCAO MO SCF (6-31G and 6-31G\* basis sets), and semi-empirical (AM1 and PM3) methods. We also calculated the distribution of the molecular electrostatic potentials (MEPs) on the Van der Waals surfaces in order to correlate it with some measurable properties of the compounds.

## Results and Discussion

The 5*H*-indolo[2,3-*b*]quinoline synthetic pathways are outlined in Scheme 1. 6*H*-Indolo[2,3-*b*]quinolines **6** were synthesized by decomposition of corresponding triazoles **5** in polyphosphoric acid (PPA) at 110–160°C and then transformed into 5-methyl-5*H*-indolo[2,3-*b*]quinolines **7** by quaternization with dimethyl sulfate followed by alkalization of quaternary salts with 20% NaOH. The starting triazoles **5** were prepared either by heating with corresponding chloroquinoline **1** and with benzotriazole **2** at 110–120°C (**5d**) or by condensation (**5a–c**) substituted in benzotriazole ring) of **1** with *o*-nitroaniline derivatives **3** and by subsequent reduction of the nitro group in intermediate **4** followed by diazotization of the amines obtained. Compounds **8** and **9** have been described in literature a number of times (Schemes 1 and 2).

Our earlier investigations into the 5*H*-indolo[2,3-*b*]quinoline group indicated that all the compounds belonging to this series were partially protonated under physiological conditions.<sup>3,5</sup> Therefore the values of the dissociation constants for the novel compounds **7a–e** were deduced from their UV spectra at fixed wavelength taken in buffers at pH 2.2 to 8.3. The  $pK_a$  values ranged from 6.02 (for the C-9 mono methoxy-derivative) to 8.07 (for the dimethoxy-derivative) with an isosbestic point at 276–293 nm (Table 1). This means that, at low pH, 5*H*-indolo[2,3-*b*]quinolines occur in the form of salts and become easy soluble in water.

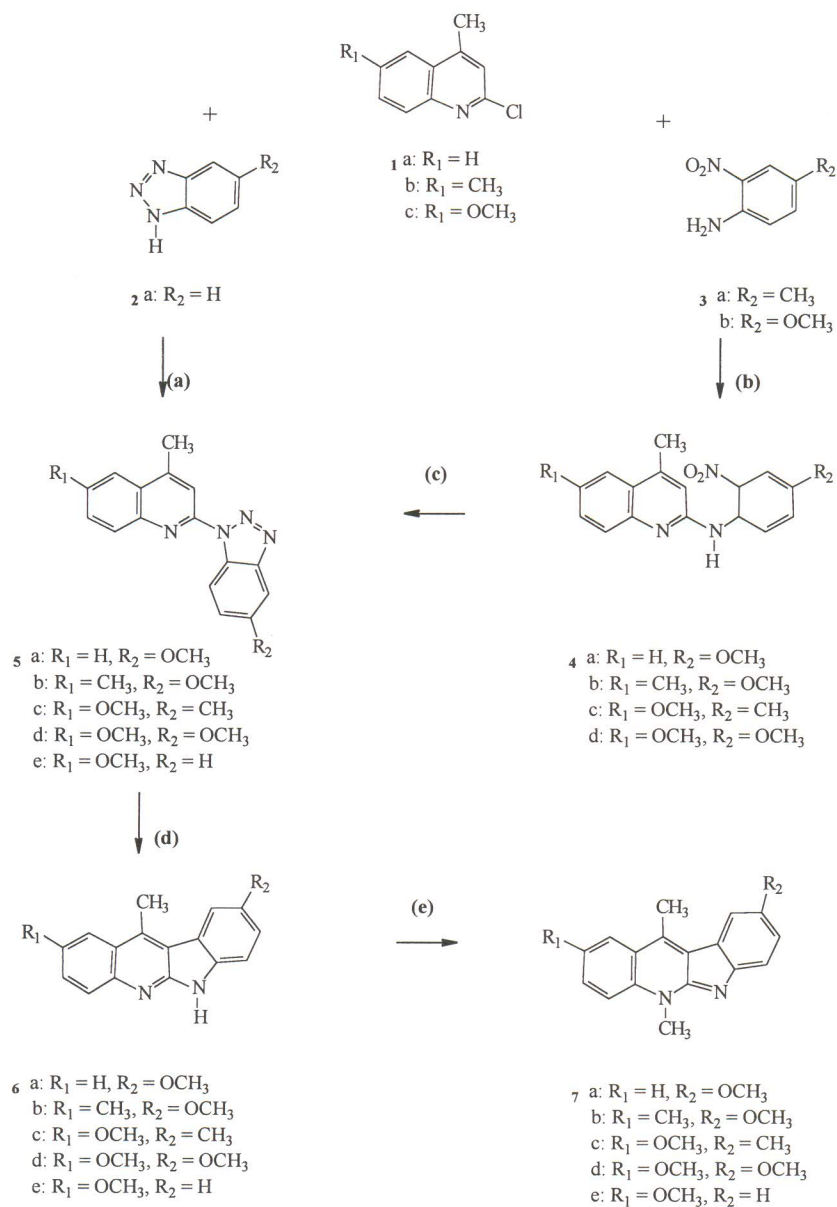
The values of the hydrophobic parameter (logP) corroborate this finding. Thus, the logP values for the compounds examined, which were positive at pH 5 and 9, became negative at pH 2.2 (Fig. 1). As we expected, it was the dimethoxy derivative (compound **7d**) that showed the highest hydrophilicity.

Like the previously tested methyl-5*H*-indolo[2,3-*b*]quinolines, compounds **7a–e** were found to display toxicity against prokaryotic and eukaryotic cells. Table 2 summarizes the antimicrobial activity of the compounds, expressed as minimum inhibitory concentration values (MICs) against the representatives of Gram-negative and Gram-positive bacteria and pathogenic fungi. All derivatives showed significant activity against Gram-positive bacteria and fungi in the MIC range 0.015 to 0.12 μM. No antimicrobial activity against Gram-negative bacteria was observed for these compounds.

The cytotoxic properties of compounds **7a–e** were determined in vitro against several human malignant lines: HL-60 promyelocytic leukemia, T-470 breast carcinoma, SW-707 colon adenocarcinoma, A-599 lung carcinoma, A-431 epidermal carcinoma, and BM-melanoma. All the compounds were found to be cytotoxic, ED<sub>50</sub> ranged from 0.2 to 2.48 μM. The most sensitive lines were promyelocytic leukemia HL-60 and colon adenocarcinoma SW-707. The least active compounds were our lead compound DiMIQ **8**, and ellipticine **10** (Table 3), whereas the most cytotoxic were compounds **7c**, **7d** and **9** (compound **9**, which had been selected as the most active against the KB cell line in our previous study,<sup>3</sup> was examined for comparison).

The differences in the DNA binding properties between the compounds referred to as **7a–e** were estimated by examining the increase of calf thymus DNA denaturation temperature ( $\Delta T_m$ ) in their presence and by determining the binding constants ( $K_{app}$ ). Measurements of DNA denaturation temperature were carried out at a drug: DNA ratio of 1:10 in 5 mM Tris-HCl buffer. The  $\Delta T_m$  values ranged from 12 to 19°C. For DiMIQ **8**, 2,9-dimethyl-DiMIQ **9**, and ellipticine **10** (used as control) the  $\Delta T_m$  values were found to be 11, 19, and 9.8°C, respectively (Table 4).

We found that the binding of indolo[2,3-*b*]quinolines to calf thymus DNA was accompanied by variations in the UV spectra according to the pattern reported previously.<sup>3</sup> And this finding allowed for the determination of the *r* values (mol of drug bound per mol of nucleotide) and of the *c* values (free drug concentration). The Scatchard plots were analyzed according to the McGhee and Von Hippel<sup>4</sup> model by nonlinear fitting of the data according to the equation  $r/c = K_{app} * (1 - n * r) * [(1 - n * r)/(1 - (n - 1) * r)]^{n-1}$  in order to obtain the binding constant to an isolated site and apparent site size. The DNA binding parameters were found to range from  $2.32 \times 10^6 \text{ M}^{-1}$  (for the binding constant  $K_{app}$ ) and 2.28 (for the number of nucleotides/binding site (*n*) for C-2 methoxy substituted compound **7c** to  $63.2 \times 10^6 \text{ M}^{-1}$  ( $K_{app}$ ) and 2.42 for the *n* values for dimethoxy substituted compound **7d**. In our experiments with reference indolo[2,3-*b*]quinolines: unsubstituted DiMIQ **8** and



**Scheme 1.** General scheme of synthesis of 5*H*-indolo[2,3-*b*]quinolines. Conditions: (a) 110–150°C, (b) 150–160°C; (c)  $\text{SnCl}_2/\text{HCl}$ , then  $\text{NaNO}_2/\text{HCl}$ ; (d) polyphosphoric acid, 110–160°C; (e) dimethyl sulfate, than NaOH.

dimethyl substituted compound **9**,  $K_{\text{app}}$  was  $0.23 \times 10^6 \text{ M}^{-1}$  at  $n=4.96$  and  $63.2 \times 10^6 \text{ M}^{-1}$  at  $n=2.42$ , respectively. Analogous values found for ellipticine were:  $K_{\text{app}} = 4.87 \times 10^6 \text{ M}^{-1}$  at  $n$  equal to 4.1 (Table 4).

Our previous studies regarding the DiMIQ-induced double stranded DNA breaks formation mediated by topoisomerase II implied the furtherance of our enzymatic assay *in vitro* for compounds **7a–e** under conditions established earlier.<sup>3</sup> We found that all of the 5*H*-indolo[2,3-*b*]quinolines stimulated DNA cleavage, producing a maximum of the cleavable complexes in the concentration range of 0.6 to 1.4  $\mu\text{M}$ , when purified calf thymus topoisomerase II and circular pSP65 DNA as substrate were used (Table 4).

Initially the geometry of compounds **7a–e**, DiMIQ and ellipticine was optimized by the semi-empirical AM1

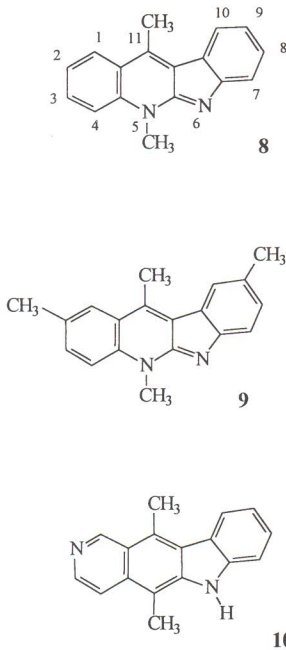
method, and some of the investigated derivatives were found to be bent (Table 5). The bending of the structure occurred between ring A and ring B (defined in Figure 2). The values of the torsional (valence) angles (also defined in Figure 2)  $\phi_1$  (C4-C4a-N5-C5a) and  $\phi_2$  (C1-C11a-C11-C10b) are listed in Table 5. As shown by these data, the most distinct bending is the one in compound **7d** (selected as the most active in the present study) and the one in compound **9** (selected previously as the most active<sup>3</sup>). Only DiMIQ **8** and ellipticine **10**

To resolve the question of planarity, the geometry of these compounds was optimized by other methods, i.e. the semi-empirical PM3 hamiltonian and the ab initio procedure involving the 6-31G and 6-31G\* basis sets. This time no significant bends were found between the A-ring and the B-ring (Table 5). Thus, the ab initio

procedure using the 6-31G\* basis set (with polarization functions) was much more reliable and confirmed the planarity of the investigated compounds. These results were also confirmed by the alternative semi-empirical PM3 approach. In this case, the bending of the indolo[2,3-*b*]quinolines observed in AM1 calculations, as well as correlation between calculated bending and

other (physicochemical and biological) properties seems to be fortuitous.

Electrostatic properties play a key role in the interaction between strongly charged DNA polymers and intercalating ligands.<sup>6</sup> These interactions are responsible for the short-range effects resulting from intercalation in a defined geometry (hydrogen bonds, stacking), and for the long-range stacking effects accounting for the sequence specific docking of the intercalator in the DNA helix. Long-range electrostatic interactions are responsible for the relative angular orientation of the molecular (DNA/intercalator) complexes. This holds



**Scheme 2.** Structures of reference compounds. (8) 5,11-dimethyl-5*H*-indolo[2,3-*b*]quinoline; (9) 2,5,9,11-tetramethyl-5*H*-indolo[2,3-*b*]quinoline; (10) ellipticine.

**Table 1.** Isosbestic points and  $pK_a$  values of compounds 7a–e<sup>a</sup>

Compd.	Isosbestic point [nm]	$pK_a$	$\lambda$ [nm]
7a	293	6.02 ± 0.09	273
7b	287	7.87 ± 0.10	304
7c	282	7.47 ± 0.10	278
7d	290	8.07 ± 0.11	285
7e	276	7.64 ± 0.11	281

<sup>a</sup> Determination of  $pK_a$  value was performed at indicated wavelength using Henderson–Hasselbach equation ( $pK_a = \text{pH} - \log ([\text{A}^-]/[\text{HA}])$ ) under conditions elaborated earlier.<sup>3</sup> Presented values are mean values of five experiments; values of standard deviation are given.

**Table 3.** Cytotoxic activity ED<sub>50</sub> ( $\mu\text{M}$ )<sup>a</sup>

Compd	Tumor cell lines					
	HL-60	T-47D	SW-707	A-549	A-431	BM
7a	n.d. <sup>c</sup>	n.d.	0.90 ± 0.04	0.70 ± 0.03	n.d.	n.d.
7b	0.22 ± 0.03	1.25 ± 0.05	0.47 ± 0.03	1.40 ± 0.04	0.50 ± 0.02	1.35 ± 0.04
7c	0.20 ± 0.02	0.91 ± 0.05	0.47 ± 0.03	0.60 ± 0.03	0.34 ± 0.02	0.90 ± 0.03
7d	0.22 ± 0.05	1.25 ± 0.03	0.52 ± 0.04	1.60 ± 0.04	0.35 ± 0.02	0.88 ± 0.03
7e	n.d.	n.d.	2.48 ± 0.05	1.18 ± 0.03	n.d.	n.d.
8 <sup>b</sup>	1.60 ± 0.05	1.60 ± 0.03	2.70 ± 0.04	2.07 ± 0.03	1.43 ± 0.04	2.55 ± 0.05
9 <sup>b</sup>	0.40 ± 0.02	2.00 ± 0.05	0.73 ± 0.02	1.70 ± 0.02	0.57 ± 0.03	1.62 ± 0.04
10 <sup>b</sup>	1.20 ± 0.04	12.5 ± 0.1	6.40 ± 0.03	3.49 ± 0.04	2.00 ± 0.04	4.25 ± 0.05

<sup>a</sup> Cell lines: HL-60, promyelocytic leukemia; T-470, breast carcinoma; SW-707, colon adenocarcinoma; A-549, lung carcinoma; A-431, epidermal carcinoma; BM, melanoma. Presented values are mean values of nine experiments; standard deviations are given.

<sup>b</sup> Compounds 8–10 were used as a standard.

<sup>c</sup> n.d., not determined.

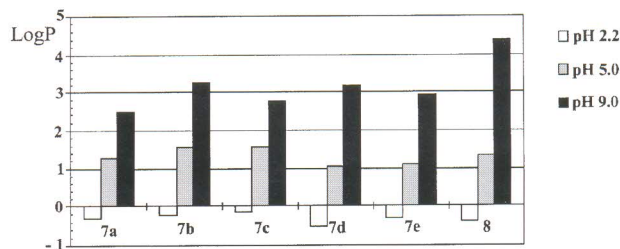


**Figure 1.** Octanol:water partition coefficient ( $\text{logP}$ ) of compounds 7aBe. Water–octanol partition coefficients were determined on pK<sub>b</sub>-100 column (4.6 × 250 mm, 42°C, 1.0 mL/min) using 0.01%  $\text{H}_2\text{SO}_4$  in methanol as mobile phase. All compounds were eluted in the well-defined peaks.  $\text{LogP}$  defined as  $\text{logP} = \log (C_f(\text{octanol})/C_f(\text{water}))$ . Presented values are mean values of five experiments.

**Table 2.** Antimicrobial activity MIC (mM)<sup>a</sup>

Compd	Strains					
	1	2	3	4	5	6
7a	n.a. <sup>c</sup>	n.a.	0.12	0.06	0.06	0.12
7b	n.a.	n.a.	0.03	0.06	0.03	0.03
7c	n.a.	n.a.	0.03	0.015	0.015	0.015
7d	n.a.	n.a.	0.03	0.03	0.12	0.12
7e	n.a.	n.a.	0.06	0.03	0.03	0.12
8 <sup>b</sup>	n.a.	n.a.	0.12	0.06	0.03	0.06

<sup>a</sup> Strains used: 1. *Escherichia coli* PCM 271; 2. *Pseudomonas aeruginosa* PCM 499; 3. *Staphylococcus aureus* PCM 458; 4. *Micrococcus luteus* PCM 525; 5. *Candida albicans* (clinical isolate); 6. *Trichophyton mentagrophytes* (clinical isolate). MICs were determined at the concentration range of 0.01 to 5 mM.

<sup>b</sup> Compound 8 was used as a standard.

<sup>c</sup> n.a., no activity (MIC > 5 mM).

**Table 4.** Interaction of compounds **7a–e** with calf thymus DNA and DNA topoisomerase II

Compd.	$\Delta T_m^a$	$\lambda$ (nm) <sup>b</sup>	$K_{app}$ ( $M^{-1}$ ) ( $\times 10^6$ )	$n$	$CC_{max}$ ( $\mu M$ ) <sup>c</sup>	% CC
<b>7a</b>	12.0 ± 0.3	344.0	2.35 ± 0.43	2.31 ± 0.09	1.4 ± 0.1	18 ± 1
<b>7b</b>	14.6 ± 0.1	345.0	17.4 ± 4.92	2.57 ± 0.07	1.0 ± 0.1	30 ± 1
<b>7c</b>	15.3 ± 0.2	347.0	2.32 ± 0.32	2.28 ± 0.08	0.8 ± 0.1	32 ± 2
<b>7d</b>	19.0 ± 0.3	350.0	63.2 ± 0.00	2.42 ± 0.00	0.6 ± 0.1	35 ± 2
<b>7e</b>	12.4 ± 0.4	350.0	6.20 ± 1.22	2.71 ± 0.12	1.2 ± 0.1	20 ± 1
<b>8<sup>d</sup></b>	11.0 ± 0.2	340.0	0.23 ± 0.77	4.96 ± 0.1	5.0 ± 0.1	22 ± 1
<b>9<sup>d</sup></b>	19.0 ± 0.4	345.0	39.48 ± 0.76	2.83 ± 0.14	0.4 ± 0.1	24 ± 1
<b>10<sup>d</sup></b>	9.8 ± 0.3	301.0	1.44 ± 0.70	5.53 ± 0.28	<i>n.d.<sup>e</sup></i>	<i>n.d.</i>

<sup>a</sup> Increase ( $\Delta T_m$ ) of calf-thymus DNA denaturation temperature. Measurements were taken in 5.0 mM pH 7.0 Tris-HCl buffer containing 50 (M) calf thymus DNA (Boehringer-Mannheim, average molecular weight  $1.2 \times 10^6$  D) 50  $\mu M$  EDTA, 5.0 (M drug, 5% DMSO).

<sup>b</sup> Binding constant values ( $K_{app}$ ) and  $n$  values (nucleotide/binding site) were calculated from Schatchard plot using McGhee and von Hippel<sup>4</sup> model of DNA-ligand interaction. Measurements were taken at indicated wavelength, by titration of the 10  $\mu M$  solution of drug with 1.33 mM solution of DNA.

<sup>c</sup> Topoisomerase II-induced DNA cleavage ( $CC_{max}$ ) by indolo[2,3-*b*]quinolines. Measurements were taken according to a previously elaborated procedure.<sup>3</sup>

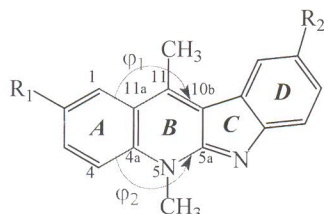
<sup>d</sup> Compounds **8–10** were used as a standards.

<sup>e</sup> *n.d.*, not determined; standard deviations are given.

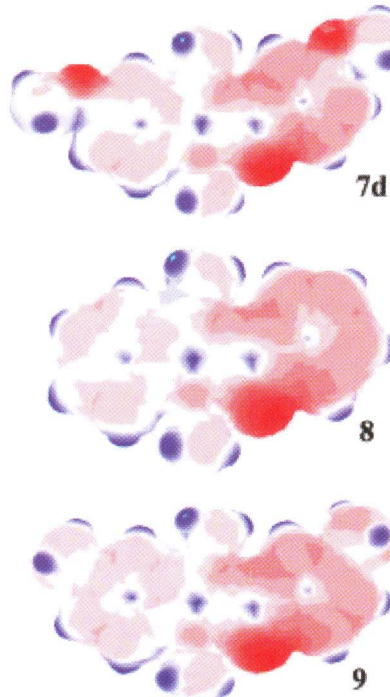
**Table 5.** Torsional angles of optimized indolo[2,3-*b*]quinolines

Compd	AM1		PM3		6-31G		6-31G*	
	$\varphi_1$	$\varphi_2$	$\varphi_1$	$\varphi_2$	$\varphi_1$	$\varphi_2$	$\varphi_1$	$\varphi_2$
<b>7a</b>	180.0	-179.8	179.7	-179.7	-179.9	179.9	180.0	180.0
<b>7b</b>	-179.9	-179.9	176.8	-177.1	180.0	179.0	180.0	180.0
<b>7c</b>	-179.8	179.7	177.1	176.4	180.0	180.0	180.0	180.0
<b>7d</b>	-167.2	168.2	178.9	-178.8	180.0	180.0	180.0	180.0
<b>7e</b>	179.7	-179.8	177.1	-176.4	179.9	-179.9	180.0	180.0
<b>8<sup>a</sup></b>	179.6	-179.7	179.7	-179.7	180.0	179.9	180.0	180.0
<b>9<sup>a</sup></b>	-162.6	167.9	179.7	-179.6	-179.9	179.9	180.0	180.0
<b>10<sup>a</sup></b>	179.6	-179.9	179.1	-176.6	180.0	180.0	180.0	180.0

<sup>a</sup> Compounds **8–10** were used as a standard.

**Figure 2.** Geometry of 5*H*-indolo[2,3-*b*]quinolines. Torsional angles  $\varphi_1$  C1-C11a-C-11-C10b, and  $\varphi_2$  C4-C4a-N5-C5a.

not only for hydrogen-bonded systems<sup>7</sup> but also for sandwich complexes of aromatic molecules.<sup>8</sup> Such specific interactions could be reasonably described by multipole expansions<sup>7–9</sup> representing the anisotropy of the molecular charge distribution at the atomic level. The specific electronic properties of intercalating molecules may be visualized by the molecular electrostatic potential (MEP) plotted at Van der Waals surfaces.<sup>10</sup> Such simple model of electrostatic properties describes the anisotropy of the molecular charge distribution. Higher multipole moments introduced to the MEP model may bring about significant changes in the surface MEP distribution<sup>10</sup> and could be related to some properties of the molecules (lipophilicity, long-range interactions, ligand – receptor binding constant, etc.). The MEP surfaces obtained for DiMIQ and for the most active 2,9-dimethoxy-derivative **7d** form quite similar patterns (Fig. 3). In both cases, strongly negative potentials (free electron

**Figure 3.** Molecular Electrostatic Potential (MEP) on the Van der Waals surfaces for selected indolo[2,3-*b*]quinolines. (7d) 2,9-dimethoxy-5,11-dimethyl-5*H*-indolo[2,3-*b*]quinoline; (8) 5,11-dimethyl-5*H*-indolo[2,3-*b*]quinoline; (9) 2,5,9,11-tetramethyl-5*H*-indolo[2,3-*b*]quinoline.

pairs occurring in base-forms of the compounds) are located near the N-6 atom and shifted outside towards the D-ring (yellow spots), whereas weaker potentials are located near N-5. The MEP surface near the external hydrogen atoms in the A-ring (H-1, H-2, H-3, H-4) is more positive (green spots) than the MEP surfaces near the D-ring protons (H-7, H-8, H-9, H-10). The negative potential above the molecular plan is shifted toward the C-ring and the D-ring, which parallels the charge shift.

The MEP maps obtained for other investigated compounds do not differ very much from one another (data not shown). This suggests, that in our case, it is not so much the electrostatics as the geometry of the molecule that can be regarded as responsible for the differences in the physicochemical and biological properties.

### Conclusion

The results of the study allow the following generalizations to be made: (i) introduction of two methoxy group into the indolo[2,3-*b*]quinoline system increases the water-solubility of the compound, (ii) the presence of substituents at C-2 and/or C-9 accounts for an increase of the denaturation temperature of calf thymus DNA, and (iii) the contribution of the position character and number of substituents in the aromatic area of indolo[2,3-*b*]quinolines to the calf thymus DNA affinity becomes distinct. The highest  $K_{app}$  values are found for di-substituted (C-2 and C-9) dimethoxy (and dimethyl) derivatives. This is correlated with their cytotoxic activities in vitro; (iv) the presence of substituents at C-2 and/or C-9 also brings about an increase of cytotoxic activity as compared to the lead compound (DiMIQ); (v) each compound produces in vitro calf thymus topoisomerase II-induced cleavable complexes of pSP65 DNA. The most cytotoxic compounds stimulate the most efficiently formation of topoisomerase II-mediated DNA breaks; (vi) methoxy (and methyl) substituents at C-2 and C-9 presumably account for a bending of the indolo[2,3-*b*]quinoline system (as we found using the semi-empirical AM1 method for geometry optimization). This bending is likely to be responsible for the manner of DNA helix unwinding, as well as for the manner by which topoisomerase recognizes the changes induced in the DNA helix; (vii) there is very likely to be an interplay between the character of the substituent, its influence on the shape of the molecule and the quality of the intercalator.

### Experimental

#### Chemistry

Melting points were taken in open capillary tubes on a Köfler-type apparatus and were uncorrected.  $^1\text{H}$  NMR spectra were recorded on a Varian Gemini 200 (200 MHz) spectrometer. Chemical shifts are expressed in ppm, using TMS as an internal standard. The IR spectra were taken in KBr pellets, using a Beckman 4240 spectrometer. UV spectra were recorded in dioxane with a Beckman Acta M-VI spectrometer. MS spectra were obtained with an Inectra AMD-604 apparatus ( $-70\text{ eV}$ ).

Elemental microanalyses were performed by the Analytical Laboratory of the Wrocław University of Technology (symbols of the analyzed elements are given only if the element was within 0.4% of the theoretical value). Column chromatography was carried out using Merck Kieselgel 60 (230–400 mesh). The purity and identity of the compounds were checked out by TLC, using Merck DC-Alufolien Kieselgel F<sub>254</sub>. Abbreviations: DMF = dimethylformamide; PPA = polyphosphoric acid.

**Synthesis of 4-methyl-2-(2-nitroanilino)quinolines 4a-d:** general procedure. The equimolar mixture of chloroquinoline **1**<sup>11,12</sup> and nitroaniline **3** was stirred at 150–160°C for 10 h, then cooled and crystallized from ethanol containing 10% of ammonia.

**2-(4-Methoxy-2-nitroanilino)-4-methylquinoline (4a).** Yield 53%; mp 148–150°C; IR v 3400, 1505 cm<sup>-1</sup>. Anal. (C<sub>17</sub>H<sub>15</sub>N<sub>3</sub>O<sub>3</sub>): C, H, N.

**2-(4-Methoxy-2-nitroanilino)-4,6-dimethylquinoline (4b).** Yield 81%; mp 169–174°C; IR v 3300, 1590, 1500, 1450, 1270, 1215, 1200 cm<sup>-1</sup>. Anal. (C<sub>18</sub>H<sub>17</sub>N<sub>3</sub>O<sub>3</sub>): C, H, N.

**6-Methoxy-4-methyl-2-(4-methyl-2-nitroanilino)quinoline (4c).** Yield 81%; mp 146–154°C; IR v 3315, 1620, 1605, 1570, 1525, 1360, 1215, 1205, 1175, 1150 cm<sup>-1</sup>. Anal. (C<sub>18</sub>H<sub>17</sub>N<sub>3</sub>O<sub>3</sub>): C, H, N.

**6-Methoxy-2-(4-methoxy-2-nitroanilino)-4-methylquinoline (4d).** Yield 96%; mp 150–156°C; IR v 3330, 1520, 1510, 1280, 1220, 1210, 1180, 1140 cm<sup>-1</sup>. Anal. (C<sub>18</sub>H<sub>17</sub>N<sub>3</sub>O<sub>4</sub>): C, H, N.

**Synthesis of 2-(5-substituted-benzotriazol-1-yl)quinolines 5a-d: general procedure.** Compound **4** (1 mol) was added portionwise to the cooled solution of SnCl<sub>2</sub> (5 mol) in 36% HCl (1.2 L) and ethanol (200 mL). The mixture was then heated in a steam bath for 30 min, and refrigerated overnight. The precipitate was collected, stirred in 20% KOH (2 L) for 30 min, and filtered off. After drying it was dissolved in a mixture of 15% HCl:ethanol 1:1 (3 L) and diazotized at 0–5°C with a solution of NaNO<sub>2</sub> (76 g, 1.1 mol) in water (0.5 L). The solid product was collected and crystallized from DMF.

**2-(5-Methoxybenzotriazol-1-yl)-4-methylquinoline (5a).** Yield 58%; mp 161–165°C; IR v 1500, 1310 cm<sup>-1</sup>. Anal. (C<sub>17</sub>H<sub>14</sub>N<sub>4</sub>O): C, H, N.

**2-(5-Methoxybenzotriazol-1-yl)-4,6-dimethylquinoline (5b).** Yield 45%; mp 234–237°C; IR v 1605, 1505, 1310, 1105, 1050, 820 cm<sup>-1</sup>. Anal. (C<sub>18</sub>H<sub>16</sub>N<sub>4</sub>O): C, H, N.

**6-Methoxy-4-methyl-2-(5-methylbenzotriazol-1-yl)quinoline (5c).** Yield 60%; mp 196–198°C; IR v 1520, 1270, 1235, 1090, 1045, 900, 820 cm<sup>-1</sup>. Anal. (C<sub>18</sub>H<sub>16</sub>N<sub>4</sub>O): C, H, N.

**6-Methoxy-2-(5-methoxybenzotriazol-1-yl)-4-methylquinoline (5d).** Yield 41%; mp 197–199°C; IR v 1525, 1505, 1425, 1310, 1240, 1120, 1055, 1035, 920, 830 cm<sup>-1</sup>. Anal. (C<sub>18</sub>H<sub>16</sub>N<sub>4</sub>O<sub>2</sub>): C, H, N.

**2-(Benzotriazol-1-yl)-6-methoxy-4-methylquinoline (5e).**<sup>13</sup> The mixture of 2-chloro-6-methoxy-4-methylquinoline (**1c**) (97.0 g, 0.5 mol) was heated until an exothermic reaction occurred (110°C). Then it was stirred without heating. The reaction temperature rose up to 140°C. When the reaction terminated, the solid was crystallized from DMF–water to give compound **5e**; yield 105.0 g (72%); mp 160–162°C (lit.<sup>13</sup> 163°C).

**Synthesis of 6H-indolo[2,3-*b*]quinolines 6a–d: general procedure.** The corresponding triazole **5** (0.1 mol) was suspended in PPA (150 mL) and the mixture was heated at 110–160°C, until gas evolution ceased. The mixture was then cooled to 90°C, poured into iced water (1.5 L) and the precipitate was further cooled. After washing with water the precipitate was heated in a steam bath in 25% NH<sub>3</sub> (500 mL), filtered off, washed with water, crystallized from pyridine and recrystallized from DMF.

**9-Methoxy-11-methyl-6H-indolo[2,3-*b*]quinoline (6a).** Yield 14%, mp 283–285°C, NMR (DMSO-*d*<sub>6</sub>) δ 11.25 (bs, 1H), 8.34 (d-d, 1H, *J*=8.5–1 Hz), 7.94 (d-d, 1H, *J*=8.5–1 Hz), 7.83 (d, 1H, *J*=2.5 Hz), 7.70 (d-d-d, 1H, *J*=9.7–1.5 Hz), 7.50 (d-d, 1H, *J*=7–1.5 Hz), 7.42 (d, 1H, *J*=8.5 Hz), 7.18 (d-d, 1H, *J*=9–2.5 Hz), 3.90 (s, 3H), 3.18 (s, 3H); IR ν 3250–2700, 1670, 1490 cm<sup>-1</sup>; MS (*m/e*, rel intensity) 262 (77, M<sup>+</sup>), 247 (100). Anal. (C<sub>17</sub>H<sub>14</sub>NO): C, H, N.

**9-Methoxy-2,11-dimethyl-6H-indolo[2,3-*b*]quinoline (6b).** Yield 14%, mp above 300°C, NMR (DMSO-*d*<sub>6</sub>) δ 11.71 (bs, 1H), 8.15 (bs, 1H), 7.88 (d, 1H, *J*=8.6 Hz), 7.82 (d, 1H, *J*=2.5 Hz), 7.61 (d-d, 1H, *J*=8.6–1.5 Hz), 7.45 (d, 1H, *J*=8.6 Hz), 7.18 (d-d, 1H, *J*=8.8–2.5 Hz), 3.90 (s, 3H), 3.18 (s, 3H), 2.56 (s, 3H); IR ν=3160–2840, 1600, 1490, 1265, 1220, 815 cm<sup>-1</sup>; MS (*m/e*, rel intensity) 276 (80, M<sup>+</sup>), 261 (100). Anal. (C<sub>18</sub>H<sub>16</sub>N<sub>2</sub>O): C, H, N.

**2-Methoxy-9,11-dimethyl-6H-indolo[2,3-*b*]quinoline (6c).** Yield 30%, mp above 300°C, NMR (DMSO-*d*<sub>6</sub>) δ 11.67 (bs, 1H), 8.15 (s, 1H), 7.90 (d, 1H, *J*=9 Hz), 7.61 (d, 1H, *J*=2.6 Hz), 7.46–7.39 (m, 2H), 7.34 (d-d, 1H, *J*=8.3–1.1 Hz), 3.96 (s, 3H), 3.17 (s, 3H), 2.52 (s, 3H); IR ν 3180–2860, 1640, 1250, 1230, 1195, 825, 730 cm<sup>-1</sup>; MS (*m/e*, rel intensity) 276 (100, M<sup>+</sup>), 261 (67), 233 (66). Anal. (C<sub>18</sub>H<sub>16</sub>N<sub>2</sub>O): C, H, N.

**2,9-Dimethoxy-11-methyl-6H-indolo[2,3-*b*]quinoline (6d).** Yield 21%, mp above 252°C (decomp.), NMR (DMSO-*d*<sub>6</sub>) δ 11.33 (s, 1H), 7.85 (d, 1H, *J*=9.2 Hz), 7.81 (d, 1H, *J*=2.4 Hz), 7.58 (d, 1H, *J*=2.8 Hz), 7.40 (d, 1H, *J*=8.7 Hz), 7.38 (d-d, 1H, *J*=9.2–2.8 Hz), 7.16 (d-d, 1H, *J*=8.7–2.5 Hz), 3.96 (s, 3H), 3.90 (s, 3H), 3.14 (s, 3H); IR ν 3180–2810, 1650, 1500, 1280, 1230, 830 cm<sup>-1</sup>; MS (*m/e*, rel. intensity) 292 (90, M<sup>+</sup>), 277 (100). Anal. (C<sub>18</sub>H<sub>16</sub>N<sub>2</sub>O<sub>2</sub>): C, H, N.

**2-Methoxy-11-methyl-6H-indolo[2,3-*b*]quinoline (6e).**<sup>13</sup> Yield 25%, mp 305–307°C.

**Synthesis of 5,11-dimethyl-6H-indolo[2,3-*b*]quinoline 7a–d: general procedure.** The corresponding 6H-indolo[2,3-*b*]quinoline **6** (0.01 mol) and dimethyl sulfate (1.5 mL) in toluene (20 mL) were heated in a sealed tube at

150–160°C for 12 h. After cooling the precipitate was collected, washed with acetone and added to 20% NaOH (50 mL). The mixture was then extracted with CHCl<sub>3</sub>, the extract was dried over MgSO<sub>4</sub> and chromatographed on a silica gel column. The orange product **7** was eluted with CHCl<sub>3</sub>, the solvent was evaporated and the residue was recrystallized.

**9-Methoxy-5,11-dimethyl-5H-indolo[2,3-*b*]quinoline (7a).** Yield 30%, mp 206–207°C (from toluene), NMR (CDCl<sub>3</sub>-*d*<sub>1</sub>) δ 8.17 (d-d, 1H, *J*=9–1 Hz), 7.77–7.64 (m, 4H), 7.44 (d-d-d, 1H, *J*=8–6–2 Hz), 7.16 (d-d, 1H, *J*=9–2.5 Hz), 4.25 (s, 3H), 3.92 (s, 3H), 3.08 (s, 3H); IR ν 1635, 1495, 1475, 1465, 1215 cm<sup>-1</sup>; UV ( $\lambda_{\text{max}}$ , log ε) 291 nm (4.66); MS (*m/e*, rel intensity) 276 (56, M<sup>+</sup>), 261 (100). Anal. (C<sub>18</sub>H<sub>16</sub>N<sub>2</sub>O): C, H, N.

**9-Methoxy-2,5,11-trimethyl-5H-indolo[2,3-*b*]quinoline (7b).** Yield 53%, mp 160–165°C (from toluene:hexane), NMR (CDCl<sub>3</sub>-*d*<sub>1</sub>) δ 7.90 (bs, 1H), 7.66 (d, 1H, *J*=2.5 Hz), 7.64 (d, 1H, *J*=8.5 Hz), 7.55 (m, 2H), 7.15 (d-d, 1H, *J*=8.5–2.5 Hz), 4.22 (s, 3H), 3.91 (s, 3H), 3.03 (s, 3H), 2.54 (s, 3H); IR ν 1645, 1505, 1480, 1220, 1150, 830 cm<sup>-1</sup>; UV ( $\lambda_{\text{max}}$ , log ε) 292 nm (4.70); MS (*m/e*, rel intensity) 290 (47, M<sup>+</sup>), 275 (100). Anal. (C<sub>19</sub>H<sub>18</sub>N<sub>2</sub>O): C, H, N.

**2-Methoxy-5,9,11-trimethyl-5H-indolo[2,3-*b*]quinoline (7c).** Yield 47%, mp 168–174°C (from toluene:hexane), NMR (CDCl<sub>3</sub>-*d*<sub>1</sub>) δ 7.93 (bs, 1H), 7.64 (d, 1H, *J*=9 Hz), 7.61 (d, 1H, *J*=1.5 Hz), 7.50 (d, 1H, *J*=2.5 Hz), 7.40–7.32 (m, 2H), 4.28 (s, 3H), 3.95 (s, 3H), 3.02 (s, 3H), 2.55 (s, 3H); IR ν 1645, 1500, 1490, 1480, 1475, 1240, 1225 cm<sup>-1</sup>; UV ( $\lambda_{\text{max}}$ , log ε) 291 nm, 4.73; MS (*m/e*, rel intensity) 290 (100, M<sup>+</sup>), 275 (42). Anal. (C<sub>19</sub>H<sub>18</sub>N<sub>2</sub>O): C, H, N.

**2,9-Dimethoxy-5,11-dimethyl-5H-indolo[2,3-*b*]quinoline (7d).** Yield 39%, mp 165–171°C (from toluene:hexane); NMR (CDCl<sub>3</sub>-*d*<sub>1</sub>) δ 7.66 (m, 2H), 7.61 (d, 1H, *J*=2.5 Hz), 7.51 (d, 1H, *J*=2.5 Hz), 7.38 (d-d, 1H, *J*=9–2.5 Hz), 7.16 (d-d, 1H, *J*=9–2.5 Hz), 4.28 (s, 3H), 3.97 (s, 3H), 3.92 (s, 3H), 3.00 (s, 3H); IR ν 1640, 1630, 1500, 1480, 1460, 1230, 1220, 1040 cm<sup>-1</sup>; UV ( $\lambda_{\text{max}}$ , log ε) 294 nm (4.66); MS (*m/e*, rel intensity) 306 (50, M<sup>+</sup>), 291 (100). Anal. (C<sub>19</sub>H<sub>18</sub>N<sub>2</sub>O<sub>2</sub>): C, H, N.

**2-Methoxy-5,11-dimethyl-5H-indolo[2,3-*b*]quinoline (7e).**<sup>13</sup> Yield 55%, mp 149–150°C.

#### Determination of pK<sub>a</sub>

The pK<sub>a</sub> values of 5*H*-indolo[2,3-*b*]quinolines were deduced from their UV absorption spectra. Measurements were performed on a Pharmacia LKB Biochrom Bio-4060 spectrophotometer, by a method elaborated earlier.<sup>3</sup> The spectra of the drugs (dissolved in DMSO) were recorded in 0.02 M phosphate buffers pH 2.2, 5.35, 7.10, 8.30, in a 1 cm pathlength cuvette at 25°C. The final concentration of DMSO was 5%.

#### Determination of lipophilicity

The logP values for individual compounds were estimated by the microscale-flask method combined with

HPLC analysis of both water (buffer) and octanol phase. A detailed description of the procedure was published elsewhere.<sup>3</sup>

### Antimicrobial activity study

MIC values were determined by serial dilution (according to a routine) method.<sup>15</sup>

### Cell cytotoxicity assay

The HL60 cell line was grown in an RPMI 1640 medium supplemented with 10% FCS (fetal calf serum). The A431 cell line was maintained in an MEM- $\alpha$  medium enriched with 10% FCS. The remaining cell lines were cultured in an opti-MEM medium supplemented with 5% FCS. All culture media also contained penicillin (50  $\mu$ g/mL), streptomycin (50  $\mu$ g/mL) and fresh L-glutamine (2 mM). All cell lines were incubated at 37°C in a humidified atmosphere of 95% air and 5% CO<sub>2</sub>. The concentration of the drugs giving 50% growth inhibition (ED<sub>50</sub>) were determined according to the MTT procedure.

### Determination of $\Delta T_m$

Experiments were carried out, using a Cary 3 Varian spectrometer equipped with a DNA Thermal Application Program according to the Cory method.<sup>14</sup>

### Determination of binding constants ( $K_{app}$ )

Measurements were carried out using a Pharmacia LKB Biochrom Bio-4060 spectrophotometer in a 5 cm path-length cuvette, at indicated wavelength, by subsequent adding of 5  $\mu$ L of 1.33 mM DNA (in 0.025 M acetate buffer pH 5.0) to 10.0 mL of 10  $\mu$ M solution of drug (in 0.025 M acetate buffer pH 5.0, and 5% of DMSO). Binding constant values ( $K_{app}$ ) and  $n$ -values (nucleotide/binding site) were calculated from the Scatchard plot, using the McGhee and von Hippel<sup>4</sup> model of the DNA-ligand interaction. Binding constants were evaluated, in terms of the Marquardt procedure of nonlinear regression, using  $K_{app} = 1.0 \times 10^6 [M^{-1}]$  and  $n = 2.0$  as starting values, and  $\Delta ss = 1.0 \times 10^{-8}$  as a final parameter of optimization.

### Determination of topoisomerase II inhibitory activity

Measurements were performed using a previously elaborated procedure<sup>3</sup> (%CC, percent of generated pSP65 DNA cleavable complexes versus total pSP65 DNA quantity).

### Quantum chemistry calculations

All structures were first optimized with semiempirical AM1, and PM3 approaches and then *ab initio* the LCAO

MO SCF method (6-31G, and 6-31G\* basis sets).<sup>16</sup> Geometry was optimized in vacuum, using steepest-descent optimization algorithm for the free base form of the drug. Electronic molecular potentials were calculated from Cumulative Atomic Multipole Moments (CAMM), derived from corresponding wavefunctions and visualized by the mol17 program.<sup>17</sup>

### Acknowledgements

The research was partially supported by the Polish State Committee for Scientific Research. We wish to thank the Wrocław Centre of Networking & Supercomputing (WCSS Grant No. 10/96) as well as the Molecular Modelling Laboratory (KBN Grant No. 6 P04A 060 09) for providing CPU time and software.

### References

1. Kaczmarek, L.; Balicki, R.; Nantka-Namirski, P.; Peczyńska-Czoch, W.; Mordarski, M. *Arch. Pharm. (Weinheim)* **1988**, 321, 463.
2. Pognan, F.; Saucier, J. M.; Paoletti, C.; Kaczmarek, L.; Nantka-Namirski, P.; Mordarski, M.; Peczyńska-Czoch, W. *Biochem. Pharmacol.* **1992**, 44, 2149.
3. Peczyńska-Czoch, W.; Pognan, F.; Kaczmarek, L.; Boratyński, J. *J. Med. Chem.* **1994**, 37, 3503.
4. McGhee, J. D.; Von Hippel, P. H. *J. Mol. Biol.* **1974**, 86, 469.
5. Osiadacz, J.; Peczyńska-Czoch, W.; Kaczmarek, L.; Opolski, A. 6th International Symposium on Molecular Aspects of Chemotherapy 9–12 July 1997, Gdańsk, Poland.
6. Naray-Szabo, G.; Ferenczy, G. G. *Chem. Rev.* **1995**, 95, 829.
7. Price, S. L.; LoCelso, F.; Treichel, J. A.; Goodfellow, J. M.; Umrania, Y. *J. Chem. Soc. Faraday Trans.* **1993**, 89, 3407.
8. Price, S. L.; Stone, A. J. *J. Chem. Phys.* **1987**, 86, 2859.
9. Sokalski, W. A.; Poirier, R. *Chem. Phys. Lett.* **1983**, 98, 86.
10. Sokalski, W. A.; Sawaryn, A. *J. Chem. Phys.* **1987**, 87, 526.
11. Campbell, K. N.; Tipson, S. R.; Elderfield, R. C.; Campbell, B. K.; Clapp, M. A.; Gensler, W. J.; Morisson, D.; Moran, W. *J. Org. Chem.* **1946**, 11, 803.
12. Kaslow, C. E.; Laver, W. M. *Org. Synt. Coll. 3*, 194.
13. Holt, S. J.; Petrov, V. *J. Chem. Soc.* **1948**, 922.
14. Cory, M.; McKee, D. D.; Kagan, J.; Henry, D. W.; Miller, A. *J. Am. Chem. Soc.* **1985**, 107, 2528.
15. Approved standard M7-A2, In *National Committee for Clinical Laboratory Standards*, 2nd ed.; Villanova, PA, 1990.
16. Frish, M. J.; Trucks, G. W.; Schlegel, H. B.; Gill, P. M. W.; Johnson, B. G.; Robb, M. A.; Cheesman, J. R.; Keith, T. A.; Petersson, G. A.; Montgomery, J. A.; Raghavachari, K.; Al-Laham, M. A.; Zakrzewski, V. G.; Ortiz, J. V.; Foresman, J. B.; Cioslowski, J.; Stefanov, B. B.; Nanayakkara, A.; Challacombe, M.; Peng, C. Y.; Ayala, P. Y.; Chen, W.; Wong, M. W.; Andres, J. L.; Replogle, E. S.; Gomperts, R.; Martin, R. L.; Fox, D. J.; Binkley, J. S.; Defrees, D. J.; Baker, J.; Stewart, J. P.; Head-Gordon, M.; Gonzales, C.; Pople, J. A. Gaussian 94 (Revision 3.1), Gaussian, Inc., Pittsburgh, PA, 1995.
17. Sokalski, W. A.; Sneddon, S. *J. Mol. Graphics* **1991**, 9, 86.